



Original paper

## Delta<sup>4</sup> Discover transmission detector: A comprehensive characterization for in-vivo VMAT monitoring

Edoardo Petrucci<sup>a</sup>, Lorenzo Radici<sup>a</sup>, Valeria Casanova Borca<sup>a</sup>, Silvia Ferrario<sup>b</sup>,  
Marina Paolini<sup>b</sup>, Massimo Pasquino<sup>a,\*</sup>

<sup>a</sup> Medical Physics Department, A.S.L. TO4, 10015 Ivrea, TO, Italy

<sup>b</sup> Radiotherapy Department, A.S.L. TO4, 10015 Ivrea, TO, Italy



## ARTICLE INFO

## Keywords:

IMRT quality assurance  
In-vivo delivery monitoring  
Transmission detector

## ABSTRACT

**Objective:** To investigate the dosimetric behaviour, influence on photon beam fluence and error detection capability of Delta<sup>4</sup> Discover transmission detector.

**Methods:** The transmission detector (TRD) was characterized on a TrueBeam linear accelerator with 6 MV beams. Linearity, reproducibility and dose rate dependence were investigated. The effect on photon beam fluence was evaluated in terms of beam profiles, percentage depth dose, transmission factor and surface dose for different open field sizes. The transmission factor of the 10x10 cm<sup>2</sup> field was entered in the TPS's configuration and its correct use in the dose calculation was verified recalculating 17 clinical IMRT/VMAT plans. Surface dose was measured for 20 IMRT fields. The capability to detect different delivery errors was investigated evaluating dose gamma index, MLC gamma index and leaf position of 15 manually modified VMAT plans.

**Results:** TRD showed a linear dependence on MU. No dose rate dependence was observed. Short-term and long-term reproducibility were within 0.1% and 0.5%. The presence of the TRD did not significantly affect PDDs and profiles. The transmission factor of the 10x10 cm<sup>2</sup> field size was 0.985 and 0.983, for FF and FFF beams respectively. The 17 recalculated plans met our clinical gamma-index passing rate, confirming the correct use of the transmission factor by the TPS. The surface dose differences for the open fields increase for shorter SSDs and greater field size. Differences in surface dose for the IMRT beams were less than 2%. Output variation ≥2%, collimator angle variations within 0.3°, gantry angle errors of 1°, jaw tracking and leaf position errors were detected.

**Conclusions:** Delta<sup>4</sup> Discover shows good linearity and reproducibility, is not dependent on dose rate and does not affect beam quality and dose profiles. It is also capable to detect dosimetric and geometric errors and therefore it is suitable for monitoring VMAT delivery.

## Introduction

Intensity modulated radiation therapy (IMRT) and Volumetric modulated arc therapy (VMAT) allow to better conform dose to target volumes than traditional 3D conformal radiation therapy while minimizing dose to adjacent normal tissues. Consequently, they have become the predominant radiotherapy techniques for a variety of treatment sites. The steep dose gradients generated by means of variations in multileaf collimator motion, gantry rotation speed and dose rate have increased type and frequency of potential errors. Consequently, extensive quality assurance program (QA) to be appropriate for the treatment technology used are needed. In most of the radiation oncology

departments, QA programs consist of two components: AAPM TG-100 [1] and AAPM TG-142 [2] methodology for machine QA, that ensures that each component of the delivery system is working within tolerance, and a patient-specific pre-treatment IMRT QA, that checks the accuracy of IMRT plan dose calculation and detects relevant errors in the radiation delivery. IMRT and VMAT techniques require an extensive quality assurance program for treatment delivery, including, in addition to traditional pre-treatment QA, in-vivo [3–5] or real time monitoring systems [6–8].

Along with detector arrays [9], electronic portal imaging devices [10,11] and delivery log-file analysis [12,13], transmission detectors (TRD) can be used to perform in-vivo monitoring and verification of the

\* Corresponding author.

E-mail address: [mpasquino@aslto4.piemonte.it](mailto:mpasquino@aslto4.piemonte.it) (M. Pasquino).

<https://doi.org/10.1016/j.ejmp.2021.04.017>

Received 26 January 2021; Received in revised form 13 April 2021; Accepted 18 April 2021

Available online 1 May 2021

1120-1797/© 2021 Associazione Italiana di Fisica Medica. Published by Elsevier Ltd. All rights reserved.



Fig. 1. Delta<sup>4</sup> Discover mounted on the TrueBeam Linac head (left) and slid out while remaining fixed to the gantry (right).

delivery process over the course of treatment. TRDs based on wedge shaped ionization chambers [14], multiwire ionization chambers [15,16], diodes [17,18] and scintillating fibers [19] have been developed with the aim to provide an accurate verification of the dose delivered to the patient on a fraction by fraction basis. However, there are some significant concerns about the use of this type of detectors for dosimetric measurements: the potential collision issues during treatment, the perturbation of the beam fluence, the need to account for the beam attenuation in the TPS, the increase in surface dose and finally the cost/benefit ratio.

The aim of the study was to complement previous investigations [20–22] of the high resolution diode based TRD Delta4 Discover (ScandiDos, Uppsala, Sweden) for its implementation in clinical workflow. This work evaluates the dosimetric behavior in terms of linearity and reproducibility, dependence of the signal from dose rate, influence on photon beam fluence and contribution to surface dose. Additionally, considering the importance to know the error detection capabilities of an IMRT QA system used in clinical environment for in-vivo verification of VMAT delivery, we investigated the ability of the system to detect errors intentionally introduced in arc VMAT plans.

## Materials and methods

The Delta<sup>4</sup> Discover transmission detector is a fluence measurement device designed to monitor the fidelity of the dose distribution delivered during every treatment [21,22]. The detector consists of 4040p-type diode detectors each with an active area of 1 mm diameter and separated by 2.5 mm and 5 mm along and perpendicular to the multileaf collimator (MLC) motion direction respectively. The diode array can measure a maximum field size of  $25 \times 19.5 \text{ cm}^2$  when projected to the isocenter level. The detector can be easily attached to the head of a TrueBeam Linac (Varian Medical Systems, Palo Alto, CA, USA) (Fig. 1), extending 2.3 cm from its collimator [23].

When the detector is attached to the Linac's head, the Interface Mount detects TRD's presence (via switches activated by TRD itself) and validates its presence by reading its identification code and comparing it with the accessory identified in the treatment plan loaded for treatment. If validation is not successful, the Linac system will not allow Beam On.

When used by itself, in the so-called *Express Measure Mode*, the Delta<sup>4</sup> Discover can only provide information on the position of the MLC leaves, gantry and collimator that compares to the values derived from the treatment plan. However, to monitor the accuracy of the dose delivered at each fraction of treatment delivery, the fluence measurements have to be converted in dose ones. To this aim, the device has to be used in the so-called *Synthesis Mode*, in conjunction with the Delta<sup>4</sup> Phantom+ [24] (ScandiDos, Uppsala, Sweden), a diode array that directly measures the dose for each control point, in order to create a link between the signal level from both devices. This preliminary synchronization allows one to

use the Delta<sup>4</sup> Discover alone during treatment and to synthesize fluence measurements into a dose distribution in the Delta<sup>4</sup> Phantom+. In such a way, the Delta<sup>4</sup> Discover can be used to verify, by means of the gamma analysis implemented in the detector's software, the dose distribution at each fraction of treatment delivery and the cumulative dose delivery of a modulated arc treatment as a function of control point.

Additionally, for each leaf that can be tracked, the detector integrates the diodes' signal typically over 25 ms and sends that integrated signal to the PC. For each of those packages the actual gantry angle is measured and the leaf edges are computed. A histogram of leaf deviations between the measured leaf edge and the planned MLC leaf edge position is plotted for each beam, leaf bank, control point and leaf; average and maximum deviations are reported as well. However, especially when the MLC leaves are moving very fast, the comparison of measured MLC leaf edges with planned ones in a control point may result in large but sometimes not significant MLC deviations. To overcome this issue, in analogy with the dose deviation gamma index [25], the Delta<sup>4</sup> Discover software calculates for each arc plan an MLC gamma index, by using the gamma formula and incorporating the measured difference in MLC leaf location corresponding to dose deviation and the difference in measured gantry angle corresponding to the spatial coordinate. The MLC gamma index calculation checks if the measured MLC leaf edge position intersects with an ellipsoid representing the acceptance criteria for gantry angle and leaf position deviation, that we set equal to  $1^\circ$ -1 mm, that are our clinical criteria, and  $0.5^\circ$ -0.5 mm, to investigate the TRD's response to even more stringent criteria. For each leaf bank the MLC gamma index is plotted for each control point and leaf.

Finally, gantry and collimator angle and patient-to-detector-distance are measured during treatment by means of an integrated gyroscope and a laser pointer, respectively.

The detector software enables the user to set pass or fail criteria that may be used to support the decision if a plans passes or fails the verification process. In particular, pass/fail criterion can be set for the percentage of diodes with the gamma index less than 1, percentage of MLC leaves in all control points with the MLC gamma index less than 1, deviation between planned and measured leaf tip, deviation between planned and measured collimator angle at a specific gantry angle and deviation between planned and measured distance between patient surface and Delta<sup>4</sup> Discover's Distance meter.

The initial setup of the TRD consists in three steps. A relative calibration using a single photon energy is performed to check that all diodes operate correctly and eventually switch off the detectors with strong deviating signal (near zero or saturation). Then a detector position calibration tool checks that the diode rows of the Delta<sup>4</sup> Discover matrix are correctly centered under the MLC leaves. If the calculated position is not as expected, fine adjustment of the TRD has to be done. Finally, for each photon modality, using an IMRT plan supplied by the manufacturer, a leaf edge calibration is performed. During this

measurement the exact position of the TRD matrix along the MLC leaf trajectory and the dosimetric leaf gap is determined; these values are saved and applied later during the determination of the MLC leaf edges' position in plan verification. It seems reasonably that these procedures are periodically performed in a dedicated QA program.

All the measurements of the study were conducted on a TrueBeam linear accelerator equipped with a standard Millennium 120 multileaf collimator and all available clinically commissioned energies of 6 MV FF and 6 MV FFF.

#### Dosimetric quantities and reproducibility

The TRD's signal linearity was measured in the range 3–1000 MU, delivering a FF fixed sized field ( $10 \times 10 \text{ cm}^2$ ) at 400 MU/min on a  $30 \times 30 \times 20 \text{ cm}^3$  solid water slab phantom and extracting the TRD's central diode's signal. The same setup was used to test the dose rate dependence for a range of clinical dose rates from 60 to 600 MU/min and from 400 to 1400 MU/min, for the FF and FFF photon beam, respectively. Moreover, the TRD's response was tested over 10 consecutive measurements (short-term reproducibility) and over a period of 1 month (long-term reproducibility), normalizing the detector signal deviations to the first measurement. All the measurements were normalized to the values obtained with a Farmer ionization chamber (Type 30011, PTW Freiburg GmbH) placed centrally in the phantom, to take account of eventual fluctuations of Linac output.

#### Transmission factor and surface dose

Since the TRD is placed in the beam path between the source and the patient and could potentially impact the beam quality, percentage depth-dose curves (PDD) and dose profiles were measured with a IC13 ionization chamber (IBA Dosimetry, Schwarzenbruck, Germany) at SSD 100 cm in a Blue Phantom water tank (IBA Dosimetry, Schwarzenbruck, Germany) for all available energies, with and without the TRD mounted in the TrueBeam interface mount. PDD were acquired for  $4 \times 4$ ,  $10 \times 10$

and  $30 \times 30 \text{ cm}^2$  field sizes; in-plane and cross-plane profiles were collected at depths of  $d_{\text{max}}$  and 10 cm for the  $30 \times 30 \text{ cm}^2$  field size. Differences between the depth dose scans were evaluated in terms of depth of maximum dose  $d_{\text{max}}$  and value at 10 cm depth ( $\text{PDD}_{10\text{cm}}$ ); differences between the profiles were calculated in terms of field flatness and symmetry, in the high dose-low gradient region.

The Delta<sup>4</sup> Discover is defined in the Treatment Planning System Eclipse (Version 15.6, Varian Medical Systems, Palo Alto, CA, USA) as a tray characterized by an accessory identification code and a single specific transmission factor for each beam energy. Consequently, the TRD's transmission factor was measured for field sizes of  $3 \times 3$ ,  $4 \times 4$ ,  $5 \times 5$ ,  $8 \times 8$ ,  $10 \times 10$ ,  $12 \times 12$ ,  $15 \times 15$ ,  $18 \times 18$ ,  $20 \times 20$  and  $25 \times 25 \text{ cm}^2$  at 10 cm depth in a  $30 \times 30 \times 20 \text{ cm}^3$  solid RW3 slab phantom (PTW Freiburg GmbH), 90 cm SSD, 100 MU delivered, using a Pin-Point ionization chamber (Type 31006, PTW Freiburg GmbH) for field size up to  $4 \times 4 \text{ cm}^2$  and Farmer ionization chamber (Type 30011, PTW Freiburg GmbH) for greater field sizes. The transmission factor of the  $10 \times 10 \text{ cm}^2$  field was entered in the TPS's accessory configuration. To verify whether the TPS takes correct account of the TRD's transmission factor in the dose calculation process, 17 representative clinical IMRT/VMAT plans (10 for FF and 7 for FFF) were recalculated after introducing the measured transmission factor in the TPS. Then plans were delivered to a Delta<sup>4</sup> Phantom+ with and without the transmission detector in place. The differences between the gamma-index passing rate were evaluated using 2%–2 mm  $\gamma$ -criteria (dose difference-distance to agreement) and 10% dose cutoff threshold, that are the criteria we use in the clinical routine.

A Markus plane-parallel ionization chamber (Type 23343, PTW Freiburg GmbH), without buildup cap, was positioned at the surface and  $d_{\text{max}}$  in the solid RW3 phantom for surface dose measurements [26]. Measurements were acquired with 100 MU for  $3 \times 3$ ,  $4 \times 4$ ,  $5 \times 5$ ,  $8 \times 8$ ,  $10 \times 10$ ,  $12 \times 12$ ,  $15 \times 15$ ,  $18 \times 18$ ,  $20 \times 20$  and  $25 \times 25 \text{ cm}^2$  field sizes at 80, 90, and 100 cm SSD, with and without the transmission detector. The measurements with the transmission detector in the path of the beam were scaled using the transmission factor. The difference between

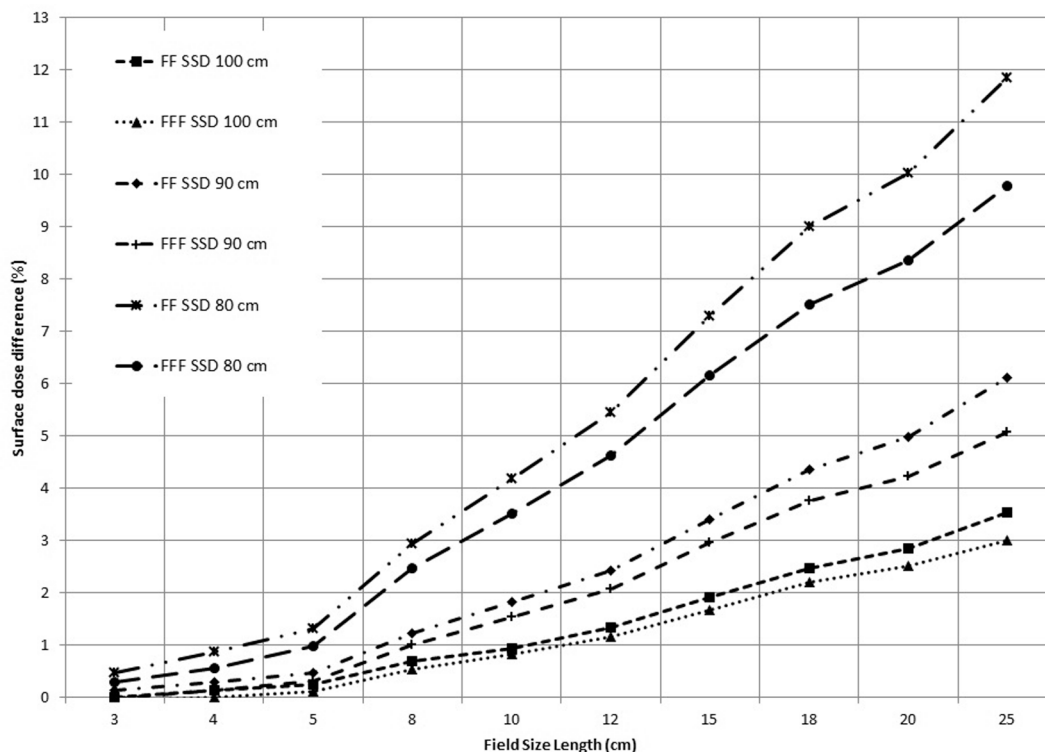


Fig. 2. Percentage surface dose difference with and without Delta<sup>4</sup> Discover for 6MV FF and 6MV FFF beams.

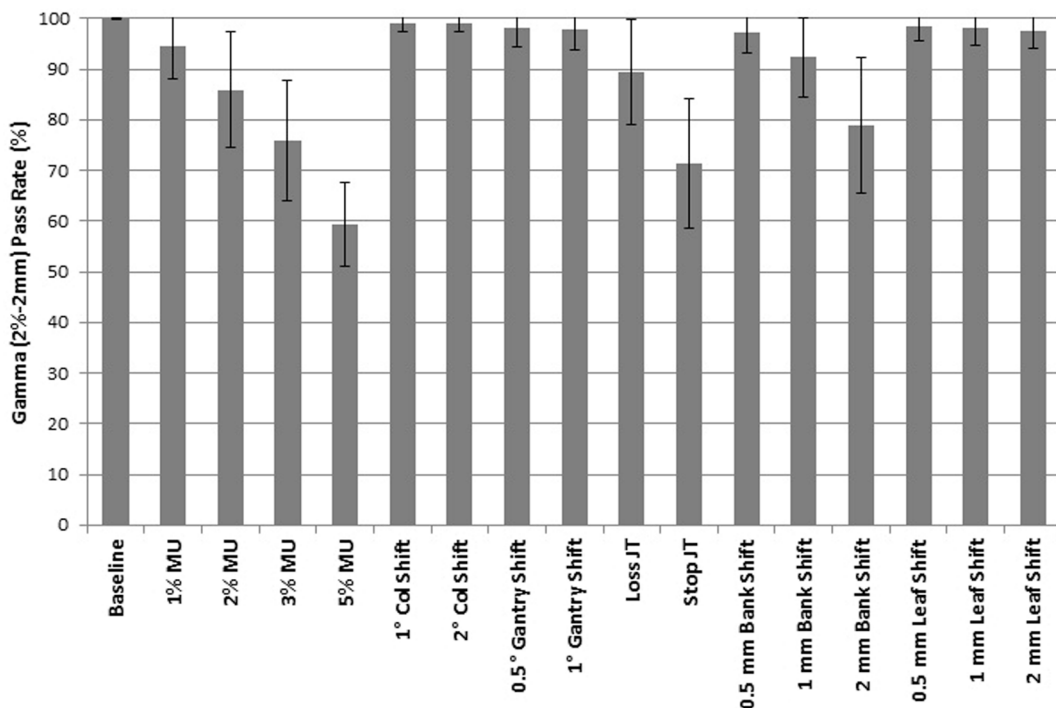


Fig. 3. Baseline Delta<sup>4</sup> Phantom+ measured gamma pass rates and synthesis predicted gamma pass rates for all modifications of the baseline VMAT plans.

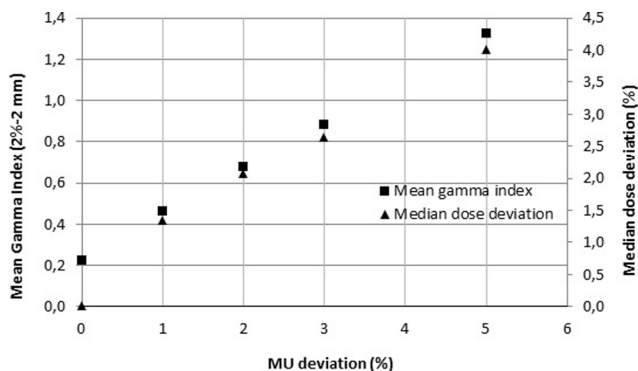


Fig. 4. 2%-2mm mean gamma index and median dose deviation with 1%-5% manually introduced MU deviations.

the surface dose with and without Discover was calculated. Then, the value obtained was normalized to the measurement at  $d_{max}$  without Discover. Additionally, surface dose increase was measured for 20 IMRT fields smaller than  $10 \times 10 \text{ cm}^2$  delivered with FF and FFF beams. Measurements were performed in RW3 phantom at  $0^\circ$  gantry angle and two different clinical SSD values (90 and 80 cm).

**Error detection capability**

The TRD’s sensitivity to detect and quantify errors between planning

and delivery was investigated by irradiating 15 VMAT plans (dual-arc prostate plans) with the 6MV beam and jaw tracking. Baseline treatment plans were created in the Eclipse TPS, exported in DICOM format and imported into the Delta<sup>4</sup> software for comparison with measurements. Baseline plans were delivered with both the Delta<sup>4</sup> Discover and Delta<sup>4</sup> Phantom+ in order to use the detector in Synthesis Mode in the subsequent measurements. Gamma analysis performed on these plans confirmed that they met the criteria used in our department for the prostate treatment (2%–2 mm for  $\gamma$ -criteria, 10% dose threshold of the global gamma evaluation and 95% for passing threshold value, chosen according to the AAPM TG 218 [27]).

Then, different types of geometric and dosimetric errors were simulated to check the ability of the system to correctly detect potential malfunctions. To this aim, using a MatLab (MathWorks, Natick, MA) script, the original DICOM RT file of each treatment was modified to introduce a different type of errors:

- machine output errors: delivered MU 1%, 2%, 3% and 5% higher than planned;
- collimator error: shifts of  $1^\circ$  and  $2^\circ$  at each control point;
- gantry error: shifts of  $0.5^\circ$  and  $1^\circ$  at each control point;
- secondary collimator jaw tracking error: jaw tracking intentionally disabled for the field, at the beginning of the delivery (stop JT) and after 1/3 of control points (loss JT);
- MLC motion error: leaves in each control point shifted by 0.5 mm, 1 mm and 2 mm in the retraction directions; the same shifts were introduced to a single leaf in the center of the beam.

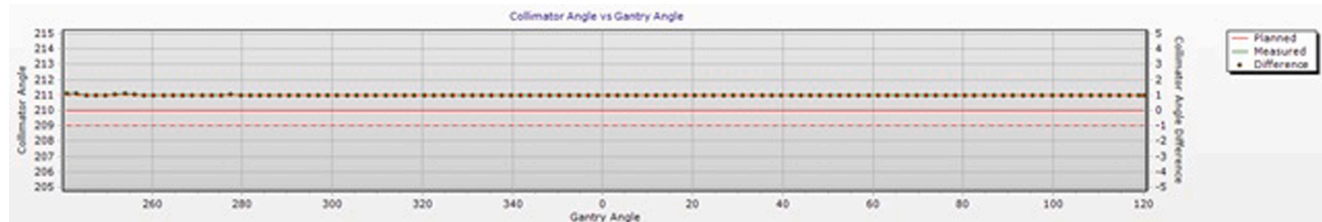


Fig. 5. Planned and measured collimator angle (and difference) versus gantry angle over the whole arc for an  $1^\circ$  introduced error.

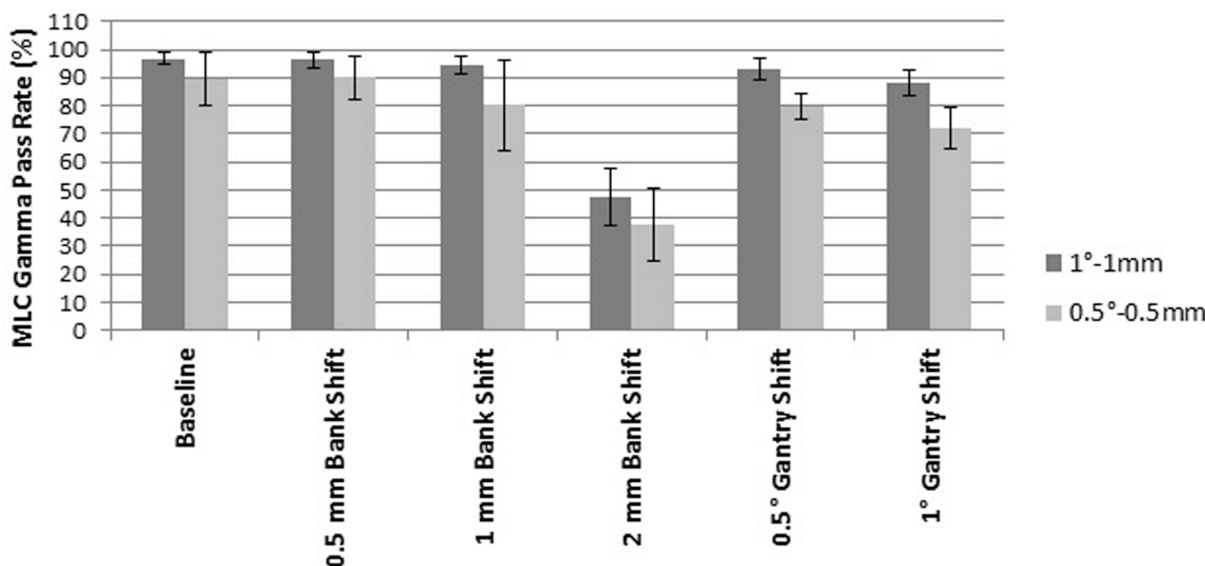


Fig. 6. MLC gamma pass rate 1°–1 mm and 0.5°–0.5 mm for gantry and leaf bank variations of the VMAT plans.

A total of 255 treatment plans and 510 VMAT arcs were then delivered using the Delta<sup>4</sup> Discover alone to evaluate the sensitivity of the system to detect the introduced errors.

**Results**

*Dosimetric quantities and reproducibility*

Delta<sup>4</sup> Discover TRD signal shows a linear dependence on MU delivered (Pearson correlation coefficient  $R^2 = 1$ ). No dependence from the dose rate was instead observed: the maximum TRD signal difference observed is 0.3% and 0.1% for FF and FFF beams, respectively.

The short-term and long-term reproducibility were within 0.1% and 0.5% respectively, for both test beams.

*Transmission factor and surface dose*

The presence of the TRD did not significantly affect depth dose curves and dose profiles: depth of maximum dose did not change by more than 1 mm; PDD<sub>10cm</sub> values did not change by more than 0.5%; maximum change in flatness was 0.4% at 10 cm depth; maximum change in symmetry was 0.2% at the depth of  $d_{max}$ .

The transmission factor of the 10x10 cm<sup>2</sup> field size was 0.985 and 0.983, for FF and FFF beams respectively. The largest difference in transmission factor relative to the 10x10 cm<sup>2</sup> field size was 0.2% and 0.1% for FF and FFF respectively. As stated above, the transmission factor of the 10x10 cm<sup>2</sup> field size was used in the TRD's configuration in the Eclipse TPS.

Regarding the measurements performed to verify whether the TPS correctly accounts for the presence of the detector both in the optimization and final dose calculation step, all the recalculated IMRT/VMAT plans passed our clinical passing rate threshold of 95% and the differences between the passing rate of the measurements performed with and without the transmission detector were less than 0.3% for all cases.

As shown in Fig. 2, the measured surface dose differences for the open square fields increase for shorter SSDs and greater field size. Furthermore, for the same SSD the surface dose increase is greater for FF beams than FFF ones. The smallest field size showed differences in surface dose less than 0.5% for both the FF and FFF beams. For the 10x10 cm<sup>2</sup> field size, the largest differences were within 1% at 100 cm SSD and 4% at 80 cm SSD; for the 25x25 cm<sup>2</sup> field size, the largest difference was of about 10% and 12% at 80 cm SSD for FFF and FF

beams, respectively.

The percentage difference of the surface dose for the IMRT beams was on average less than 1% and 2%, at 90 and 80 cm SSD respectively, for both FF and FFF beams; maximum differences were equal to 1.5% and 3.6%, respectively.

*Errors detection capability*

Fig. 3 shows the baseline Delta<sup>4</sup> Phantom+ measured gamma pass

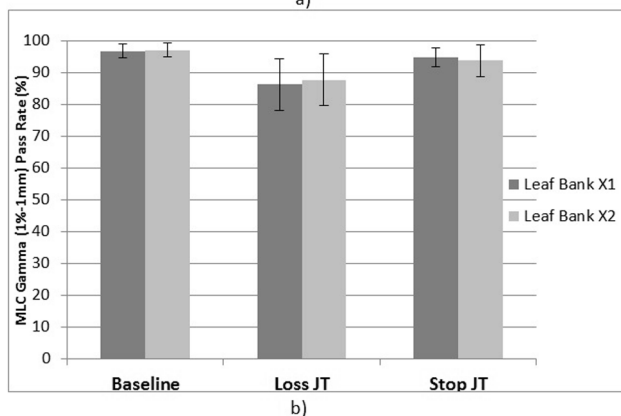
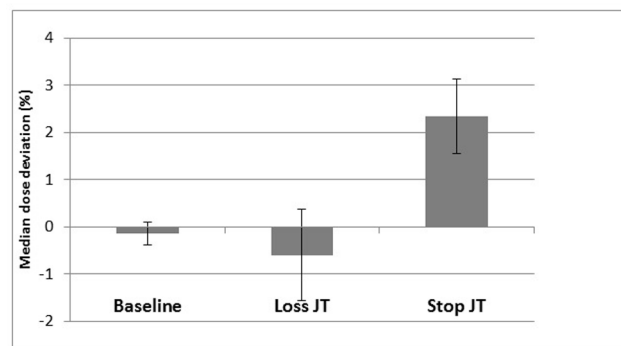


Fig. 7. Median dose deviation (a) and MLC gamma pass rate for each leaf bank (b) for the baseline plans and the error-bearing ones when jaw tracking was intentionally disabled during the delivery (Loss JT) and when it was disabled at the beginning of irradiation (Stop JT).

rates and synthesis predicted gamma pass rates for all modifications of the baseline VMAT plans.

**Monitor units**

As illustrated in Fig. 3, the dose error-bearing plans showed an average gamma passing rate significantly lower than the unmodified plans when a MU error greater than 1% was simulated. Linac output simulated error greater than 2% were always detected when using the standard passing gamma rate threshold of 95%.

In Fig. 4 the mean gamma value and the median dose deviation are plotted for the unmodified plans and the dose error-bearing ones. With respect to the Linac output, an error of 1% and 5% led to an average increase in the mean gamma value of 0.2 and 1.1, respectively; the average increase of the median dose was equal to 1.3% and 4.0%, respectively. The linearity of the TRD stated above was also confirmed by the linear trend of the plotted values with MU drift ( $R^2 = 0.999$  and

$R^2 = 0.974$  for mean gamma and median dose value, respectively).

**Collimator angle**

As shown in Fig. 3, the gamma pass rate did not change as the collimator angle was modified because the detector rotates with the collimator such that any collimator rotation results in no change to the fluence measured; furthermore, the information about the collimator angle is not used to recalculate the dose in Synthesis mode. However, the collimator angle was correctly measured during delivery within  $0.3^\circ$  by the integrated gyroscope. In Fig. 5 planned and measured collimator angle and difference versus gantry angle over the whole arc is illustrated, as displayed by the software, for an introduced error of  $1^\circ$ .

**Gantry angle**

As shown in Fig. 3, the baseline and synthesis predicted gamma pass rates stayed almost constant when gantry angles were changed. Instead,

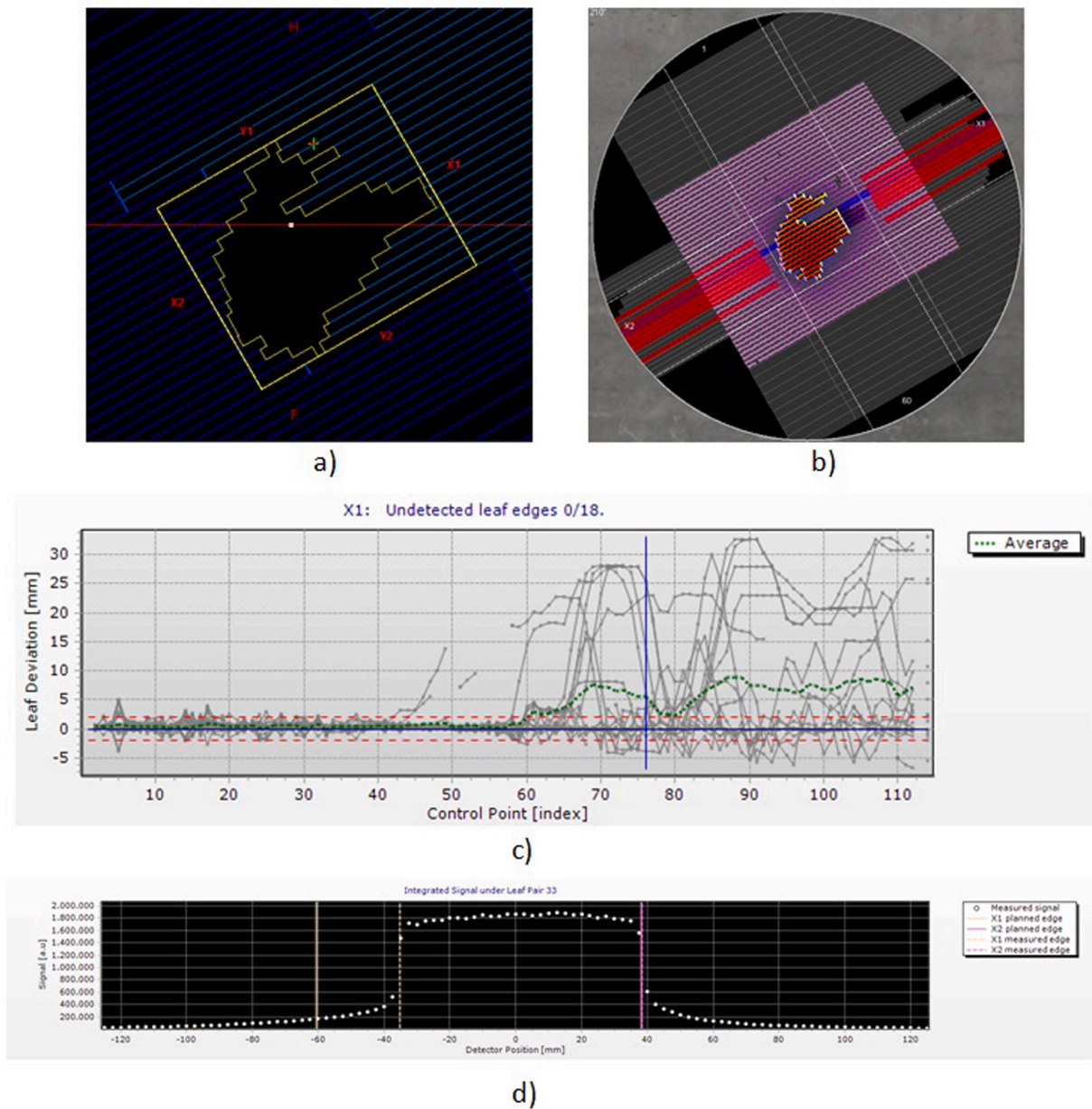


**Fig. 8.** Results of a single control point with loss of jaw tracking: a) MLC configuration in Eclipse TPS. b) All detectors and the measuring ones in the Beam's Eye View of Delta<sup>4</sup> Discover software. c) Leaf edge deviations for each control point. d) Measured and calculated leaf tips when a single control point and a MLC leaf pair is selected.

as illustrated in Fig. 6, the MLC gamma metric showed a decrease when the changes made in the baseline plan exceeded the 0.5° and 1° criteria used for the metric.

#### Jaw tracking

Fig. 3 shows the desired drop in gamma pass rates of at least 10% when jaw tracking was intentionally disabled during the delivery and of about 30% when it was disabled at the beginning of irradiation.

In Fig. 7a the median dose is plotted for the baseline plans and the error-bearing ones. In the case of loss of jaw tracking, a decrease less than 1% in the measured median dose was observed due to the in-field disabled jaw. Otherwise, the jaw tracking stopped at the beginning of the delivery outside the field produced an increase greater than 2% in the median dose due to the lack of jaws attenuation.

Instead, the MLC gamma metric shows a more noticeable drop in the gamma pass rate in each leaf bank when jaw tracking was intentionally disabled during the delivery (Fig. 7b): the percentage of plans that still pass the standard 95% gamma pass rate decreased by about 60% and 45%, in the case of Loss JT and Stop JT, respectively.

In Fig. 8 the results of a single control point with loss of jaw tracking is shown. The leaf edge detection algorithm fits a sigmoid to both signal's penumbras and determines the point of sharpest gradient of each sigmoid. This position is then adjusted with the dosimetric leaf gap as obtained during the MLC calibration to retrieve the MLC leaf edge. In this case, the edge detection of the leaves under the disabled jaw is incorrect and determines a lower MLC gamma pass rate.

#### Multi leaf collimator

As illustrated in Fig. 3, errors in the leaf position exceeding the gamma DTA criterion of 2 mm were always detected.

In Figs. 9 and 6 the average difference in leaf deviations and MLC gamma pass rates for plans with MLC bank motion errors are illustrated. The average detected difference in leaf deviations were within 0.2 mm of the actual values used in the modified plan. However, due to synchronization issues, the comparison of measured MLC leaf edges with planned ones showed misreported MLC deviations: the largest differences for individual leaves were in the order of 13 mm with about 7% more than 3.5 mm, that is the difference threshold value suggested by the AAPM TG142 [2].

For the case where only the central leaf was moved, while the average leaf shift was correctly identified as nearly zero, it is possible to detect a shift/error only when the know shift is larger than 1 mm (Fig. 10a and 10b). As expected, the synthesis predicted gamma pass rates (Fig. 3) and MLC gamma pass rates for the plans where only one central leaf was moved did not change compared to baseline.

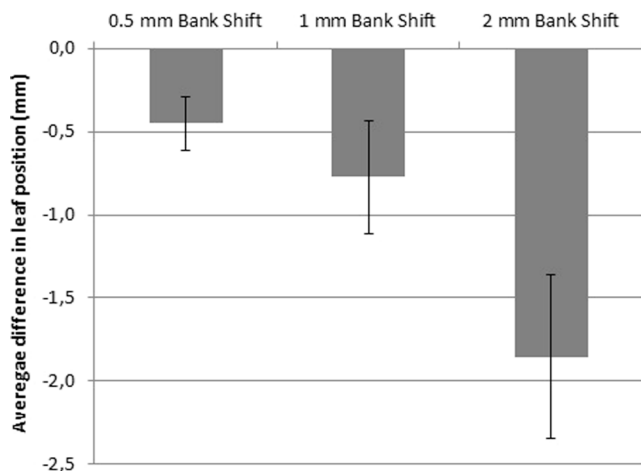


Fig. 9. Average difference in leaf positions for plans with MLC bank motion errors.

## Discussion

In this study, we investigated the performance of the Delta<sup>4</sup> Discover transmission detector system: dosimetric characteristics, impact on the radiation dose received by the patient (dose transmission and surface dose contribution) and capability to detect dosimetric and geometric errors.

The transmission detector was found to be very stable in terms of linearity ( $R^2 = 1$ ) and short and long term reproducibility (<1%); the dose rate dependence was less than 0.4% up to typical dose rate values of 6 MV FFF treatments (1400 MU/min). The results confirm that the detector can be used for both conventional and stereotactic treatment quality assurance.

Our measurements demonstrate that the presence of the transmission detector in the beam path does not affect neither the percentage depth dose curves nor the dose profiles for flattened and unflattened beams; therefore no modifications to the treatment planning system beam model is required for the use of the device. The results show that about 1.5% of a 6 MV beam and 1.7% of a 6 MV FFF beam is absorbed by the detector. These values are similar to those measured with the same setup by Li et al [20] (1.1% for 6MV beams) and by Paxton et al [22] (1.3% and 1.6% for 6MV and 6MV FFF beams, respectively). Instead, the Delta<sup>4</sup> Discover showed a measured transmission factor significantly lower than the values reported in literature for another commercially available transmission detector, Integral Quality Monitor (IQM, iRT, Germany), for which Islam et al [14] measured an attenuation factor of 7%, normalized to  $d_{max}$ , while Hoffman et al. [28] found an attenuation factor of 5.5%.

The transmission factor varies slightly with fields size; therefore it is sufficient to assign a transmission factor to each beam energy to account for the perturbation of the detector, as indirectly confirmed by the results of the patient-specific quality assurance measurements performed on clinical IMRT/VMAT plans.

As the increase in patient's surface dose regards, the open beam measurements showed that the effect depends on the SSD and field size value; in particular the larger the field size the greater the surface dose. It denotes that the off-axis scatter represents the main contribution and suggests using the TRD with caution when treating large fields ( $\geq 20 \times 20 \text{ cm}^2$ ). The effect was higher in the flattened beams than in the unflattened ones, probably due to the increased scatter contribution from the higher off-axis fluence and to the slightly lower energy of the FFF beams. Our results are similar to those measured in the same conditions (6 MV  $10 \times 10 \text{ cm}^2$  field at SSD = 90 cm) for the Delta<sup>4</sup> Discover by Li et al [20] (1.7%) and for the IQM by Islam et al [14] (3%).

When measured for typical IMRT fields, surface dose showed behavior similar to that for open square fields, with dose differences of about 1% increasing for different SSD's value. The TRD showed minimal effect on the clinically relevant radiation therapy beams for IMRT and VMAT treatments, as confirmed by the measurements performed with optically-stimulated luminescent dosimeters at SSD = 89 cm by Paxton et al [22].

Dose errors detection capability measurements for the faulty Linac output showed that a machine output drift greater than 2% was always detected by the TRD when using a 2%-2mm gamma criteria. Besides, the results confirm that this device can fulfill the AAPM TG-142 [2] requirement of detecting monthly output constancy to be within 2%. Furthermore, the linearity of the TRD stated above was also confirmed by the linear trend of the mean gamma value and the median dose versus MU drift.

The synthesis predicted gamma pass rate did not show variations when collimator angle was changed; however, it is possible to correctly measure the collimator angle with an integrated gyro, as illustrated in Fig. 5 and a pass/fail criterion can eventually be set for any observed collimator deviation.

The baseline and synthesis predicted gamma pass rates stayed almost constant when gantry angle was changed. The information about the

gantry angle is used when sorting the measured dose into control points to apply the correct diode angular correction factor to the dose sorted into that control point. However, the angular dependence of the Delta4 Phantom+ diodes is small [24] and so small differences in measured gantry angle will not have a significant effect on the measured absolute dose and thus the dose gamma index. Instead, the MLC gamma pass rate showed the expected decrease when the changes made in the baseline plan exceeded the criteria used for the metric.

The different tools of the TRD’s software allow the user to intercept a jaw tracking failure. When the jaws do not follow the leaves from the beginning of the irradiation (Stop JT), the malfunction caused a significant drop in the synthesis predicted gamma pass rate and median dose due to a greater overall beam transmission (see Figs. 3 and 7a).

Meanwhile, the MLC gamma pass rate did not show significant change, because the Stop JT does not affect the leaves edge detection by the TRD. When the jaw tracking is randomly disabled during the irradiation (Loss JT), the malfunction caused a drop of the MLC gamma pass rate (Fig. 7b), due to the incorrect edge detection of the leaves under the disabled jaw. Infact, as illustrated in Fig. 8b, the TRD derives the edge of the leaves that lie under the disabled jaw from the edge of the jaw itself. However, to ascribe the results to a jaw tracking malfunction, the user has to carry out a deeper analysis of the TRD response in each control point (Fig. 8c).

The results confirm that the Delta<sup>4</sup> Discover unit can detect millimeter changes in leaf positions in VMAT plans. The predicted gamma pass rate always detects errors in leaf positions exceeding the gamma

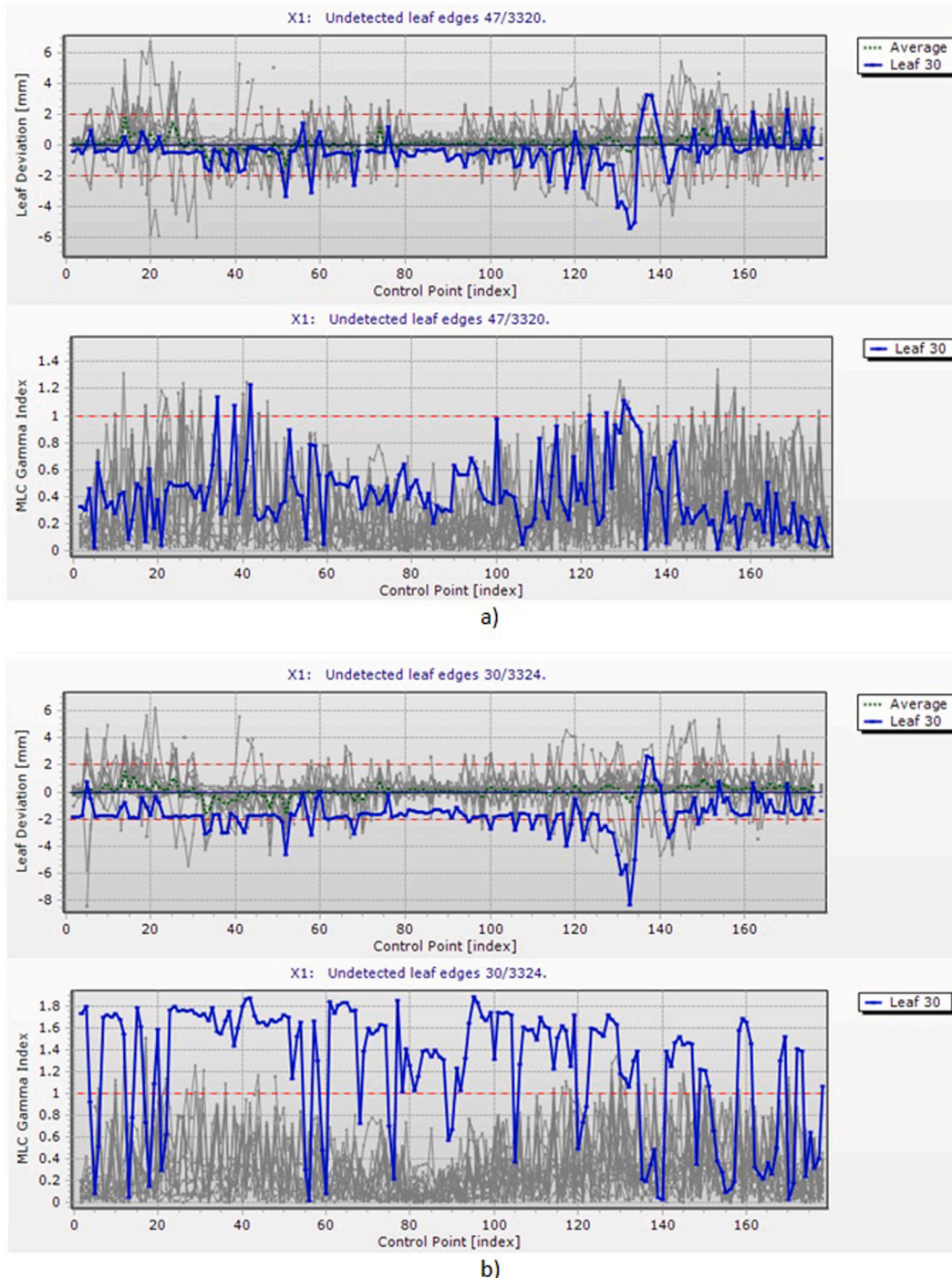


Fig. 10. Deviation between measured and planned leaf edge and MLC gamma index for each control point and leaf for 1 mm (a) and 2 mm (b) introduced shift.

DTA criterion. The software does provide the distribution of leaf deviations and offers statistics on average and maximum leaf deviations. In case of VMAT plans, the average leaf deviations were very close to the actual deviations introduced in the plans, allowing the user to detect an eventual leaf bank shift error. The results are similar to those of Sarkar et al [21], who reported an agreement between measured and introduced shifts within 0.8 mm in a single-arc VMAT plan. The observed maximum detected leaf deviation greater than 10 mm is likely due to difficulties in synchronizing measured leaf positions with planned ones where large changes are occurring in leaf position with gantry angle. Moreover, if an isolated leaf pair is nearly closed and there are large openings adjacent to these leaves, the leaf edge detection algorithm may break down. As a result, the detected leaf edges deviate significantly from the planned ones. In such cases the user shall not conclude that the treatment delivery has failed, but it will be necessary to determine whether it is reasonable that the leaves are positioned where they have been detected.

The new evaluation method available in the data analysis of the Delta<sup>4</sup> Discover software, the MLC gamma index, was confirmed to work as intended for arc plans. MLC gamma value distributions showed high consistency between errors introduced in the plan and the criteria used for the gamma calculations, as demonstrated by the significant drops when the leaf position errors started exceeding the acceptance criteria. It is important to underline that even a single leaf being incorrectly positioned was correctly identified by the system, using either the plot of the deviation between the measured and the planned MLC leaf edge or the MLC gamma index for all control points and leaves.

## Conclusion

The aim of this study was to investigate the dosimetric characteristics, the influence on photon beam fluence and the capability to detect Linac output and geometric errors of Delta<sup>4</sup> Discover transmission detector, as a propaedeutic study before implementing it in the clinical routine. The results showed that the system has good linearity and reproducibility, is not dependent on dose rate and does not affect beam quality and dose profiles. The Delta<sup>4</sup> Discover system is also capable to detect Linac output drifts, incorrect collimator and gantry angle, failure of the jaws to be positioned correctly and leaf position differences.

Last but not least: the use of the transmission detector in the clinical routine requires minimal user interaction since patient data is loaded via the direct interface to the Linac. However, some aspects need to be addressed: the loss of automatism of operation as collimator rotation or table shift, that, due to safety reasons, the Linac's technicians have to perform manually inside the bunker; the clearance's variation that can inhibit some procedures. Therefore, adequate staff training and multi-disciplinary teamwork is mandatory.

In conclusion, on the basis of our results, the Delta<sup>4</sup> Discover has been considered an effective in-vivo transmission detector for monitoring VMAT treatments delivery able to detect delivery errors and was therefore implemented in the clinical routine.

## References

- [1] Huq MS, Fraass BA, Dunscombe PB, Gibbons JP, Ibbott GS, Mundt AJ, et al. The report of Task Group 100 of the AAPM: application of risk analysis methods to radiation therapy quality management. *Med Phys* 2016;43(7):4209–62. <https://doi.org/10.1118/1.4947547>.
- [2] Klein EE, Hanley J, Bayouth J, et al. Task Group 142 report: quality assurance of medical accelerators. *Med Phys* 2009;36(9):4197–212. <https://doi.org/10.1118/1.3190392>.
- [3] Kutcher GJ, Coia L, Gillin M, Hanson WF, Leibel S, Morton RJ, et al. Comprehensive QA for radiation oncology: report of AAPM Radiation Therapy Committee Task Group 40. *Med Phys* 1994;21(4):581–618. <https://doi.org/10.1118/1.597316>.
- [4] Mijnheer B, Beddar S, Izewska J, Reft C. In vivo dosimetry in external beam radiotherapy. *Med Phys* 2013;40(7):070903. <https://doi.org/10.1118/1.4811216>.
- [5] Esposito M, Villaggi E, Bresciani S, Cilla S, Falco MD, Garibaldi C, et al. Estimating dose delivery accuracy in stereotactic body radiation therapy: a review of in-vivo measurement methods. *Radiother Oncol* 2020;149:158–67. <https://doi.org/10.1016/j.radonc.2020.05.014>.
- [6] Alber M, Broggi S, De Wagter C, et al. Guidelines for the verification of IMRT. *ESTRO booklet* 2008.
- [7] Archambault L, Briere TM, Pönisch F, Beaulieu L, Kuban DA, Lee A, et al. Toward a real-time in vivo dosimetry system using plastic scintillation detectors. *Int J Radiat Oncol Biol Phys* 2010;78(1):280–7. <https://doi.org/10.1016/j.ijrobp.2009.11.025>.
- [8] Wootton L, Kudchadker R, Lee A, Beddar S. Real-time in vivo rectal wall dosimetry using plastic scintillation detectors for patients with prostate cancer. *Phys Med Biol* 2014;59(3):647–60. <https://doi.org/10.1088/0031-9155/59/3/647>.
- [9] Essers M, Mijnheer BJ. In vivo dosimetry during external photon beam radiotherapy. *Int J Radiat Oncol Biol Phys* 1999;43(2):245–59. [https://doi.org/10.1016/s0360-3016\(98\)00341-1](https://doi.org/10.1016/s0360-3016(98)00341-1).
- [10] Mans A, Wendling M, McDermott LN, Sonke J-J, Tielenburg R, Vijlbrief R, et al. Catching errors with in vivo EPID dosimetry. *Med Phys* 2010;37(6Part2):2638–44. <https://doi.org/10.1118/1.3397807>.
- [11] Van Elmpt W, McDermott L, Nijsten S, Wendling M, Lambin P, Mijnheer B. A literature review of electronic portal imaging for radiotherapy dosimetry. *Radiother Oncol* 2008;88(3):289–309. <https://doi.org/10.1016/j.radonc.2008.07.008>.
- [12] Tyagi N, Yang K, Gersten D, Yan D. A real time dose monitoring and dose reconstruction tool for patient specific VMAT QA and delivery. *Med Phys* 2012;39(12):7194–204. <https://doi.org/10.1118/1.4764482>.
- [13] Litzenberg DW, Moran JM, Fraass BA. Verification of dynamic and segmental IMRT delivery by dynamic log file analysis. *J Appl Clin Med Phys* 2002;3(2):63–72. [https://doi.org/10.1002/\(ISSN\)1526-991410.1002/acm2.2002.3.issue-210.1120/jacmp.v3i2.2578](https://doi.org/10.1002/(ISSN)1526-991410.1002/acm2.2002.3.issue-210.1120/jacmp.v3i2.2578).
- [14] Islam MK, Norrlinger BD, Smale JR, Heaton RK, Galbraith D, Fan C, et al. An integral quality monitoring system for real-time verification of intensity modulated radiation therapy. *Med Phys* 2009;36(12):5420–8. <https://doi.org/10.1118/1.3250859>.
- [15] Poppe B, Thieke C, Beyer D, Kollhoff R, Djouguela A, Rühmann A, et al. DAVID—a translucent multi-wire transmission ionization chamber for in vivo verification of IMRT and conformal irradiation techniques. *Phys Med Biol* 2006;51(5):1237–48. <https://doi.org/10.1088/0031-9155/51/5/013>.
- [16] Poppe B, Looe HK, Chofor N, Rühmann A, Harder D, Willborn KC. Clinical performance of a transmission detector array for the permanent supervision of IMRT deliveries. *Radiother Oncol* 2010;95(2):158–65. <https://doi.org/10.1016/j.radonc.2009.12.041>.
- [17] Wong JHD, Fuduli I, Carolan M, Petasecca M, Lerch MLF, Perevertaylo VL, et al. Characterization of a novel two dimensional diode array the “magic plate” as a radiation detector for radiation therapy treatment. *Med Phys* 2012;39(5):2544–58. <https://doi.org/10.1118/1.3700234>.
- [18] Blue A, Bates R, Laing A, Maneuski D, O'Shea V, Clark A, et al. Characterisation of Vanilla—A novel active pixel sensor for radiation detection. *Nucl Instrum Methods Phys Res A* 2007;581(1-2):287–90.
- [19] Goulet M, Gingras L, Beaulieu L. Real-time verification of multileaf collimator-driven radiotherapy using a novel optical attenuation-based fluence monitor. *Med Phys* 2011;38(3):1459–67. <https://doi.org/10.1118/1.3549766>.
- [20] Li T, Wu QJ, Matzen T, Yin FF, O'Daniel JC. Diode-based transmission detector for IMRT delivery monitoring: a validation study. *J Appl Clin Med Phys*. 2016;17(5):235–244. 10.1120/jacmp.v17i5.6204.
- [21] Sarkar V, Paxton A, Kunz J, Szegedi M, Nelson G, Rassiah-Szegedi P, et al. A systematic evaluation of the error detection abilities of a new diode transmission detector. *J Appl Clin Med Phys* 2019;20(9):122–32. <https://doi.org/10.1002/acm2.v20.910.1002/acm2.12691>.
- [22] Paxton AB, Sarkar V, Kunz JN, Szegedi M, Zhao H, Huang YJ, et al. Evaluation of the effects of implementing a diode transmission device into the clinical workflow. *Phys Med* 2020;80:335–41. <https://doi.org/10.1016/j.ejmp.2020.11.017>.
- [23] <https://delta4family.com/products/at-treatment/discover/>.
- [24] Sadagopan R, Bencomo JA, Martin RL, Nilsson G, Matzen T, Balter PA. Characterization and clinical evaluation of a novel IMRT quality assurance system. *J Appl Clin Med Phys* 2009;10(2):104–19. <https://doi.org/10.1120/jacmp.v10i2.2928>.
- [25] Low DA, Harms WB, Mutic S, Purdy JA. A technique for the quantitative evaluation of dose distributions. *Med Phys* 1998;25(5):656–61. <https://doi.org/10.1118/1.598248>.
- [26] Kim S, Liu CR, Zhu TC, Palta JR. Photon beam skin dose analyses for different clinical setups. *Med Phys* 1998;25(6):860–6. <https://doi.org/10.1118/1.598261>.
- [27] Miften M, Olch A, Mihailidis D, et al. Tolerance limits and methodologies for IMRT measurement-based verification QA: Recommendations of AAPM Task Group No. 218. *Med Phys*. 2018;45(4):e53–e83. doi: 10.1002/mp.12810.
- [28] Hoffman D, Chung E, Hess C, Stern R, Benedict S. Characterization and evaluation of an integrated quality monitoring system for online quality assurance of external beam radiation therapy. *J Appl Clin Med Phys* 2017;18(1):40–8. <https://doi.org/10.1002/acm2.12014>.